Influence of Processing Conditions on Structures of 3D Ordered Macroporous Metals Prepared by Colloidal Crystal Templating

Hongwei Yan,[†] Christopher F. Blanford,[†] Justin C. Lytle,[†] C. Barry Carter,[‡] William H. Smyrl,[‡] and Andreas Stein*,[†]

Department of Chemistry, University of Minnesota, 207 Pleasant St. SE, Minneapolis, Minnesota 55455, and Department of Chemical Engineering and Materials Science, University of Minnesota, 421 Washington Ave SE, Minneapolis, Minnesota 55455

Received June 18, 2001. Revised Manuscript Received August 14, 2001

This paper presents general methods of preparing three-dimensionally ordered macroporous (3DOM) metals or alloys via templated precipitation and subsequent chemical conversion of metal salts (acetates, oxalates) within colloidal crystals of poly(methyl methacrylate) (PMMA) or polystyrene (PS) spheres. Three approaches are given to prepare 3DOM metallic Ni, Co, and Fe and the alloy $Ni_{1-x}Co_x$: (1) calcination of the metal oxalate/template composite in a nitrogen atmosphere, (2) formation of a 3DOM metal oxide followed by reduction in hydrogen, and (3) direct reduction of the metal oxalate/template composite in hydrogen. The 3DOM products obtained by these routes differ in size of the grains that compose the wall skeletons, in surface areas, and in compositions. Method 1 leads to very small grains and high surface areas but incomplete removal of carbon with graphitic layers surrounding metal grains. Method 2, as a two-step process, leads to relatively large metal grains, smaller surface areas, and carbon-free products. Method 3 strikes a compromise in these properties, with intermediate surface areas and small (<2%) amounts of remaining carbon. This paper presents synthetic details, discusses effects of the template choice (PMMA vs PS), and compares structural features of the macroporous metals and alloys, using the results of XRD, TGA, SEM, TEM, nitrogen adsorption data, and chemical analysis.

Introduction

Porous metals are important for many engineering applications, such as filters, catalysts, supports, heat exchangers, fuel cells, electrolytic cells, thermal screens, and vibration dampers.[1] In many applications, a high specific surface area is required. For porous metals prepared by conventional methods, such as powder sintering, slip foaming, slip casting, and fiber metallurgy, it is difficult to achieve high surface areas.[1] Although some microporous metals (Raney nickel)[2] or mesoporous metals (prepared from liquid crystalline phases)[3] exhibit high surface areas, a significant fraction of the pores are not easily accessible to large guests due to the relatively small pore diameters (<10 nm). Recently several preparations of porous metals formed by colloidal crystal templating techniques have been reported, which result in structures featuring three-dimensionally ordered macropores throughout the base metal.[4−13] With uniform pore sizes (typically a few hundred nanometers), bicontinuous networks, and highly accessible surface areas, these three-dimensionally ordered macroporous (3DOM) metals are anticipated to exhibit improved performance in applications, such as those requiring transport through the pores or interaction with the surface. Moreover, it has been suggested that metals with well-ordered porous networks exhibit interesting photonic properties.[14] This has been a motivating factor for the fabrication of 3DOM metals.

3DOM metals have now been prepared by several methods. For example, Jiang et al. synthesized 3DOM Ni, Cu, Ag, Au, and Pt metal films by electroless deposition within colloidal silica crystals, using nanocrystalline metals as catalysts.[5] The specific surface areas of these porous metals ranged from 9.8 to 26 m^2/

[†] Department of Chemistry.
[‡] Department of Chemical Engineering and Materials Science.

(1) Shapovalov, V. *MRS Bull.* **1994**, *19*, 24.
(2) Rausch, S.; Wendt, H. *J. Electrochem. Soc.* **1996**, *143*, 2852.
(3) Attard, G. S.; Bartlett, P. N.; Coleman, N. R. B.; Elliott, J. M.; Owen, J. R.; Wang, J. H. *Science* **1997**, *278*, 838.
(4) Yan, H.; Blanford, C. F.; Holland, B. T.; Parent, M.; Smyrl, W. H.; Stein, A. *Adv. Mater.* **1999**, *11*, 1003.
(5) Jiang, P.; Cizeron, J.; Bertone, J. F.; Colvin, V. L. *J. Am. Chem. Soc.* **1999**, *121*, 7957.
(6) Velev, O. D.; Tessier, P. M.; Lenhoff, A. M.; Kaler, E. W. *Nature* **1999**, *401*, 548.
(7) Wijnhoven, J. E. G. J.; Zevenhuizen, S. J. M.; Hendriks, M. A.; Vanmaekelbergh, D.; Kelly, J. J.; Vos, W. L. *Adv. Mater.* **2000**, *12*, 888.
(8) Miguez, H.; Meseguer, F.; Lopez, C.; Holgado, M.; Andreasen, G.; Mifsud, A.; Fornes, V. *Langmuir* **2000**, *16*, 4405.
(9) Egan, G. L.; Yu, J. S.; Kim, C. H.; Lee, S. J.; Schaak, R. E.; Mallouk, T. E. *Adv. Mater.* **2000**, *12*, 1040.
(10) Xu, L.; Zhou, W. L.; Frommen, C.; Baughman, R. H.; Zakhidov, A. A.; Malkinski, L.; Wang, J. Q.; Wiley, J. B. *Chem. Commun.* **2000**, 997.
(11) Bartlett, P. N.; Birkin, P. R.; Ghanem, M. A. *Chem. Commun.* **2000**, 1671.
(12) Tessier, P. M.; Velev, O. D.; Kalambur, A. T.; Rabolt, J. F.; Lenhoff, A. M.; Kaler, E. W. *J. Am. Chem. Soc.* **2000**, *122*, 9554.
(13) Yan, H.; Blanford, C. F.; Smyrl, W. H.; Stein, A. *Chem. Commun.* **2000**, 1477.
(14) Sievenpiper, D. F.; Sickmiller, M. E.; Yablonovitch, E. *Phys. Rev. Lett.* **1996**, *76*, 2480.

10.1021/cm0105716 CCC: $20.00
Published on Web 10/05/2001

Table 1. Synthesis Conditions for 3DOM Metals and Alloys

			calcination[b]		
metal	precursor	solvent	atmosphere	temp/°C	time
Ni	2 g of $Ni(OAc)_2 \cdot 4H_2O$	10 mL of MeOH	N_2	450	1 h
			air/H_2	400/300	3 h/2 h
			H_2	400	1h
Co	2 g of $Co(OAc)_2 \cdot 4H_2O$	10 mL of MeOH	N_2	450	1 h
			air/H_2	400/300	3 h/2 h
Fe[a]	6 g of $FeC_2O_4 \cdot 2H_2O$	5 mL of EtOH/	air/H_2	400/300	3 h/2 h
		5 mL OF H_2O/H_2O_2	H_2	400	1 h
$Ni_{1-x}Co_x$ ($x = 0.5$)	1 g of $Ni(OAc)_2 \cdot 4H_2O$	10 mL of MeOH	H_2	400	1 h
	1 g of $Co(OAc)_2 \cdot 4H_2O$				

[a] Six grams of oxalic acid was added to the mixture of $FeC_2O_4 \cdot 2H_2O$ in water. A 30% aqueous H_2O_2 solution was added dropwise until all solids were dissolved. Fe(II) oxalate was oxidized to Fe(III) oxalate by this procedure. Ethanol was added at this stage. [b] All calcinations were conducted in a 22 mm i.d. quartz tube oven at a heating rate of 2 °C/min. For the samples reduced from 3DOM metal oxides, the metal oxalate was first heated in a mixed atmosphere of air and N_2 (0.2 L min^{-1} air/1.0 L min^{-1} N_2) and then reduced in flowing H_2 (0.3 L min^{-1}). For the pure N_2 atmosphere, the flow rate was 1.0 L min^{-1}.

g. Velev et al. developed a route involving direct deposition of colloidal gold particles in colloidal crystals for preparing 3DOM gold.[6] Wijnhoven et al. also prepared 3DOM gold by electrochemical deposition.[7] Yan et al. reported the synthesis of 3DOM nickel by hydrogen reduction of a preformed macroporous oxide or by decomposition of polystyrene (PS) templated nickel oxalate in a nonoxidizing environment.[4] 3DOM nickel calcined in N_2 has a much higher surface area (122 m^2/g) than 3DOM nickel prepared from NiO reduced in H_2 (5 m^2/g). However, the former sample contains a large amount of carbon (39 wt %) due to incomplete decomposition of PS. This carbon is amorphous, and a significant fraction of the surface area may be attributed to the carbon rather than the nickel walls.

To control the carbon content and increase the structural order of 3DOM metals, we modified the templated salt precipitation method by using poly(methyl methacrylate) (PMMA) colloidal crystals instead of PS. PMMA has better wettability with polar solvents (such as H_2O and alcohol) than PS. As a consequence, metal precursor solutions involving polar solvents can infiltrate the colloidal crystals more completely, introducing fewer structural defects during the composite formation. Another reason for using PMMA instead of PS lies in its distinct thermal degradation character[15] which permits milder template removal conditions. After calcination in an appropriate atmosphere, this synthetic modification permitted the preparation of a series of metals and alloys with lower carbon content and long-range ordered arrays of macropores.

This paper provides examples for the preparation of 3DOM metallic Ni, Co, Fe, and the alloy $Ni_{1-x}Co_x$. Three approaches are given to prepare these 3DOM materials: (1) calcination of metal oxalate-infiltrated templates in nitrogen, (2) formation of a 3DOM metal oxide followed by reduction in hydrogen, and (3) direct reduction of the metal oxalate/template composite in hydrogen. The relationships between synthesis conditions and structural features of the 3DOM metals are described, using results of X-ray diffraction (XRD), thermogravimetric analysis (TGA), scanning electron microscopy (SEM), transmission electron microscopy (TEM), nitrogen adsorption data, and chemical analysis.

Experimental Section

Materials. Non-cross-linked, monodisperse PMMA spheres were synthesized using an emulsifier-free emulsion polymerization technique according to literature.[16] Depending on the experimental conditions, sphere diameters in various batches ranged from 300 to 500 nm (standard deviations ≤4%). Before use, the spheres were close-packed into colloidal crystals by gravity sedimentation or centrifugation. Manganese(II) acetate tetrahydrate (99%), cobalt(II) acetate tetrahydrate (98%), nickel(II) acetate tetrahydrate (98%), iron(II) oxalate dihydrate (99%), and oxalic acid (98%) were obtained from Aldrich. All the precursors were used as received without further purification.

Synthesis of 3DOM Metals. The procedure of the templated salt precipitation method has been described previously.[4,17] In brief, the first step was to prepare a clear precursor solution by dissolving a soluble salt of the desired metal in ethanol or methanol and removing any undissolved solid by filtration. Then close-packed PMMA colloidal crystals were soaked in this solution for 3−5 min. Excess solution was removed from the impregnated colloidal crystals by vacuum filtration. The sample was dried in air for 0.5−1 h. The theoretical volume filling fraction of the salt precursors (volume of dried salt to total volume of composite) at this stage ranged from 3% (for nickel and cobalt acetate hydrates) to 7% (for iron oxalate hydrate). The dried templated metal salt was then soaked in oxalic acid solution (ca. 3.6 g of oxalic acid in 30 mL of ethanol) for 1−2 min to form metal oxalate inside the PMMA colloidal crystals. Certain precursors, such as iron(III) oxalate, which was soluble in alcohol, could be used directly without the second precipitation step involving oxalic acid. After additional vacuum filtration and drying steps, 3DOM metals were prepared by calcining at 400−450 °C for 1−3 h in an inert or reducing atmosphere. 3DOM $Ni_{1-x}Co_x$ samples were prepared as described in ref 13. The synthesis conditions for specific samples are listed in Table 1.

Characterization. Powder XRD measurements were performed on a Siemens D5005 wide-angle XRD spectrometer with Cu Kα radiation. Average particle size determinations were based on fitting the XRD patterns by using the JADE program. TGA was performed with a Perkin-Elmer TGA-7 thermogravimetric analyzer attached to a PC via a TAC7/DX thermal controller. A Hitachi S-800 field emission SEM was used to examine the morphology of the samples. Samples for SEM were prepared by supporting 3DOM particles on an SEM stub with double-sided tape and crushing the particles with a spatula to expose internal features. TEM images were recorded using a slow-scan CCD on a Philips CM30 TEM operating at 300 kV with a LaB_6 filament. Samples for TEM were prepared by sonicating about 20 mg of the powder in 2 mL of absolute ethanol for 1 min and then depositing a drop of the suspension on a holey carbon grid. For high-temperature TEM, the sample

(15) Liggat, J. In *Polymer Handbook*; Brandrup, J., Immergut, E. H., Grulke, E. A., Eds.; Wiley: New York, 1999.
(16) Zou, D.; Ma, S.; Guan, R.; Park, M.; Sun, L.; Aklonis, J. J.; Salovey, R. *J. Polym. Sci., Part A: Polym. Chem.* **1992**, *30*, 137.
(17) Yan, H.; Blanford, C. F.; Holland, B. T.; Smyrl, W. H.; Stein, A. *Chem. Mater.* **2000**, *12*, 1134.

was dispersed in absolute ethanol by sonication, deposited onto a holey carbon film on a nickel grid, and heated in the ultrahigh-vacuum environment of the TEM column. Chemical analyses for carbon and hydrogen were carried out at Atlantic Microlabs Inc., Norcross, GA. Metals analyses for Co and Ni in 3DOM alloys were determined by inductively coupled plasma atomic emission spectroscopy (ICP-AES) by the University of Minnesota Geochemical Lab, Minneapolis, MN. Nitrogen adsorption measurements were performed on a Micromeritics ASAP 2000 V3.00 sorption analyzer. Prior to the sorption measurements, the samples were degassed under vacuum at 120 °C until a pressure ≤3 μmHg was obtained. Surface areas were calculated by the Brunauer−Emmett−Teller (BET) method.[18]

Results and Discussion

Precipitation inside the PMMA Colloidal Crystals. The templated salt precipitation method involves two steps. First, the metal acetate ($M(OAc)_x$) precursor is loaded into the interstitial space of the colloidal crystal template via a solvent carrier. Then a precipitation reaction is induced by soaking the colloidal crystals in oxalic acid solution. The second step is very important in most instances, because metal oxalate precipitates can decompose during calcination to metals, metal oxides, or metal carbonates without melting, thereby maintaining a porous structure. The final quality of the 3DOM structure depends strongly on how the precipitation reaction proceeds inside the colloidal crystals.

In the case of PS spheres, the precipitation reaction could be promoted by soaking the colloidal crystal template for a long enough time. But for PMMA, this treatment did not work because it was found that PMMA spheres dissolved in oxalic acid solution, a process which eventually ruined the ordered structure. To avoid the dissolution of PMMA, the soaking time had to be decreased to 1−2 min. Within this shortened period, it became more challenging to carry out the precipitation reaction. It was observed that, if the predeposited metal acetate inside the colloidal crystals was allowed to dry completely, as in the PS case, precipitation upon contact with the oxalic acid solution could not occur within 1−2 min, because dissolution of the metal acetate in alcohol was too slow. As a result, the ordered structure was destroyed in the calcined product due to melting of the metal acetate precursor. On the other hand, when "wet" $M(OAc)_x$/PMMA composites were placed in the oxalic acid solution without further drying, the metal acetate solution still occupied the interstitial space of the PMMA colloidal crystals, and a metal oxalate precipitate formed at the interface of the two solutions, hindering further precipitation. In this case, the ordered structure could only be found on the surface of the calcined sample. Considering the two extreme conditions, more controlled drying of the $M(OAc)_x$/PMMA composites was needed, involving addition of the oxalic acid solution to a slightly wet metal acetate deposit on the template at a time when the solution no longer blocked the channel spaces (for example, by forming a thin film on the surface of the PMMA spheres). Such an effect can be achieved by drying the composites in air at room temperature for 0.5−1 h. The exact drying conditions depended on the solvent and precursor system used. With nickel acetate and ethanol as a solvent, for example, the drying time was 1 h for millimeter-scale colloidal crystals. But with methanol as a solvent, the drying time was reduced to approximately 30 min, due to the higher volatility of methanol.

Calcination of Metal Oxalate-Filled Polymer Colloidal Crystals. All the polymer templates were removed by calcination in this work. The calcination conditions, such as heating rate, temperature, and atmosphere, have significant effects on the quality of the 3DOM structure and on the composition of the products. Because of the high porosity and thin wall thickness, the inorganic frameworks are quite fragile. Both the melting or outgassing of templates and thermal shock (i.e., uneven thermal expansion) may break the wall structure. To keep the structure as ordered as possible, a slow heating rate (e.g., 2 °C/min) should be employed to ensure a gentle process, especially at the stages when the polymer template gasifies or combusts, i.e., when a large change in volume occurs.

Another factor that influences the structural order is the grain size within the walls. For most of the investigated systems the wall skeletons are typically composed of nanocrystalline grains between ca. 5 and 40 nm in diameter. In previous work, it was noted that products with large wall grains, where the dimensions approached those of the sphere templates, tended to lose their 3D periodicity.[19] Smaller grains could be obtained with shorter calcination times at lower temperatures. However, reduced calcination times or temperatures often lead to incomplete removal of the polymer templates. Therefore, TGA measurements were employed to determine the minimum feasible temperature for template removal at a fixed heating rate. Figure 1 shows the TGA curves for pure PMMA colloidal crystals and PMMA templated nickel oxalate calcined under flowing air or N_2. For comparison, results for pure PS colloidal crystals tested under the same conditions are also provided.

When calcined in air, pure PMMA starts to lose weight abruptly at around 305 °C and is completely decomposed at about 370 °C in air (Figure 1a). In N_2, a higher temperature (415 °C) is needed to completely remove PMMA (Figure 1b). The lower decomposition temperature in air can be attributed to the combustion of polymer, which is exothermic and therefore aids the decomposition. Compared with PMMA, pure PS colloidal crystals have much higher decomposition temperatures. In air, the weight loss of PS first decreases abruptly around 450 °C and then more slowly until the temperature reaches 550 °C, when it levels off (Figure 1c). In N_2, PS starts to lose weight at around 450 °C and completely decomposes at about 510 °C (Figure 1d). The different thermal degradation characteristics for PMMA and PS are determined by their intrinsic structures. The thermal degradation of PS occurs by random scission and other mechanisms, resulting in a complex mixture of low-molecular-weight degradation products and a higher decomposition temperature.[15] In the case of PMMA, which is sterically hindered at the radical site due to the presence of the methyl substituent at the

(18) Gregg, S. J.; Sing, K. S. W. *Adsorption, Surface Area and Porosity*, 2nd ed.; Academic Press: London, 1982.

(19) Holland, B. T.; Blanford, C. F.; Do, T.; Stein, A. *Chem. Mater.* **1999**, *11*, 795.

Table 2. Structural and Compositional Parameters

metal	atmosphere	pdf file	grain size[b] (nm)	linear shrinkage[c] (%)	BET surface area (m^2/g)	element analysis C (wt %)	element analysis H (wt %)
Ni	N_2	04-0850	4.6 ± 0.3	22	162.4	14.76	0.38
	N_2[a]	04-0850	6.4 ± 0.2	23	122	38.93	0.99
	air/H_2	04-0850	25.4 ± 0.9	58	5.0	0.29	0.21
	H_2	04-0850/05-1027	23.7 ± 0.5	27	22.1	0.26	0.0
Co	N_2	15-0806	2.6 ± 0.7	19	174.7	11.64	0.70
	air/H_2	15-0806/05-0727	36.6 ± 7.2	n/a	7.8	0.38	0.0
Fe	air/H_2	06-0696	19.5 ± 0.7	55	17.9	0.30	0.0
	H_2	06-0696	39.9 ± 2.8	46	33.1	1.81	0.11
$Ni_{1-x}Co_x$ ($x = 0.5$)	H_2	N/A	33 ± 0.9	51	9.9	0.52	0.19

[a] This sample was prepared at 450 °C for 10 h in N_2, using PS colloidal crystals as a template. All other samples were prepared as outlined in Table 1 using PMMA colloidal crystals as a template. [b] Grain sizes were estimated from fwhm of diagnostic powder XRD lines. These actually correspond to average domain sizes within grains. Grain sizes observed by TEM were often ca. twice as large or larger. [c] The linear shrinkage was estimated from SEM images by ratioing the pore sizes of the products to the sphere sizes of the templates.

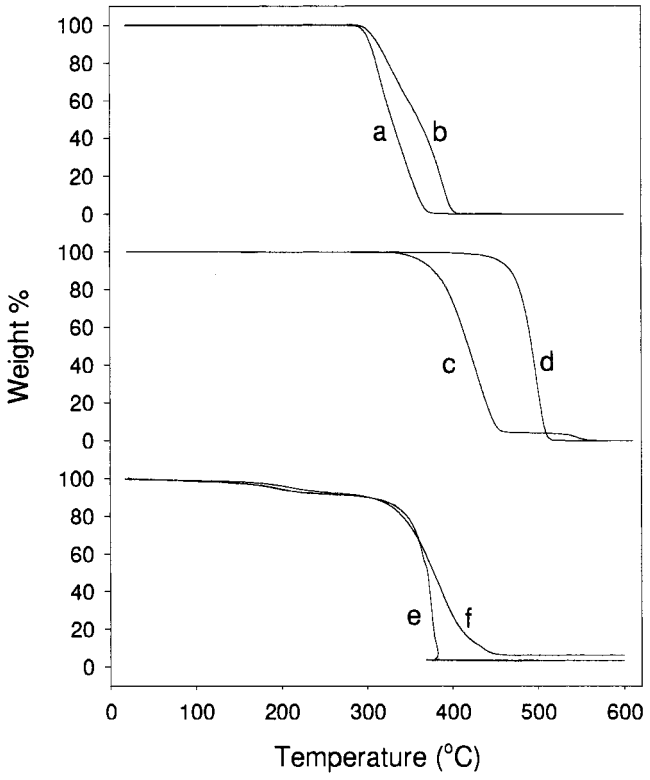

Figure 1. TGA curves for (a) PMMA calcined in air, (b) PMMA heated in nitrogen, (c) PS calcined in air, (d) PS heated in nitrogen, (e) a PMMA/nickel oxalate composite calcined in air, and (f) a PMMA/nickel oxalate composite calcined in nitrogen. Heating rates were 2 °C/min.

α-carbon site, depolymerization may proceed by an initial scission at the chain end, which results in the production of monomer.[15] From this point of view, PMMA is a better template for the synthesis of 3DOM metals and metal oxides, leading to products with a lower carbon content at a given calcination temperature.

Figure 1e shows the TGA curve for PMMA templated nickel oxalate calcined in air. Two discrete weight losses are observed in the temperature ranges between 25−250 and 300−380 °C. The first 8.5% weight loss occurs gradually and originates from the removal of residual water and solvent in the sample. The second weight loss of 87.9% occurs more suddenly and is associated with the oxidation−decomposition of the PMMA templates as well as the elimination of oxalate decomposition products. The decomposition product of nickel oxalate, mainly nickel metal, is further oxidized in air. In the case of PMMA templated nickel oxalate calcined in N_2 (Figure 1f), the first weight loss in the temperature range 25−250 °C is consistent with that in air. However, the second weight loss, which starts at 300 °C, ends at a higher temperature, 450 °C. This result indicates that it is more difficult to remove PMMA templates when the interstitial space is occupied by metal salts. The relative masses of the final products from TGA were a little higher than the theoretical values based on volume filling fractions of the salt precursors (calcination in O_2: 3.75 wt % NiO by TGA/1.8 wt % theoretical; calcination in N_2: 3.25 wt % Ni by TGA/1.4 wt % theoretical). These data indicate either that a small amount of excess, nonporous material was present on the surface of the particles or that a carbon residue was present in the case of calcination in N_2 (see below). On the basis of the TGA measurements, it can be determined that the minimum feasible calcination temperature for templated nickel oxalate is 400 °C in air and 450 °C in N_2 at the heating rates employed.

In the preparation of 3DOM metals from oxalates, the calcination atmosphere is another determining factor. Generally, the decomposition products of metal oxalates can be metals, metal oxides, or metal carbonates, depending on the electrochemical potential of the metals.[20,21] Therefore, a different atmosphere may be appropriate, depending on the specific system. For example, since the decomposition product of nickel oxalate or cobalt oxalate is metal nickel or cobalt, 3DOM Ni or Co can be synthesized directly by heating in an inert atmosphere. But for a template/iron oxalate composite, where the decomposition product is Fe_2O_3, a reducing atmosphere should be employed to obtain 3DOM Fe. In this work, three calcination strategies were used, i.e., (1) calcining metal oxalate directly in N_2, (2) calcining metal oxalate in air and then reducing the as-prepared 3DOM metal oxide in H_2, and (3) calcining metal oxalate directly in H_2. Structural and compositional parameters of the resulting 3DOM samples are summarized in Table 2. These varied significantly, depending on the processing conditions, as outlined below.

1. Thermal Treatment in an Inert Atmosphere. Some 3DOM metals, such as Ni and Co, could be synthesized directly by heating metal oxalates in an inert atmo-

(20) Robin, J. *Bull. Soc. Chim. Fr.* **1953**, 1078.
(21) Dollimore, D.; Griffiths, D. L.; Nicholson, D. *J. Chem. Soc.* **1963**, 2617.

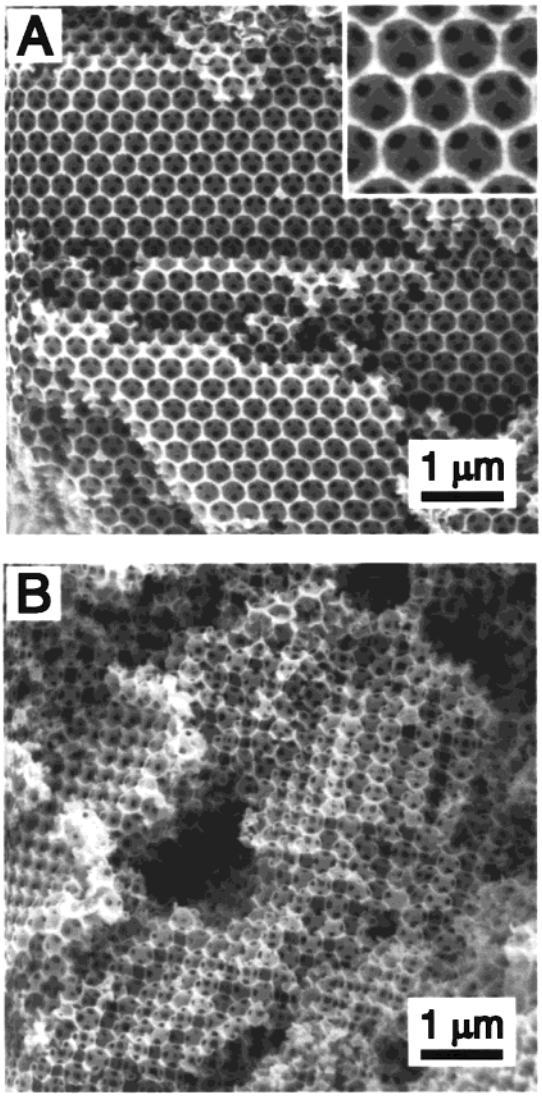

Figure 2. SEM images of (A) 3DOM Ni and (B) 3DOM Co heated in nitrogen at 450 °C for 1 h. The lighter features correspond to the metal walls that surround macropores, and the black circular features correspond to windows between adjacent macropores. The inset in image A shows an enlarged area of the 3DOM Ni sample to demonstrate the smooth, spherical appearance of the walls in this sample.

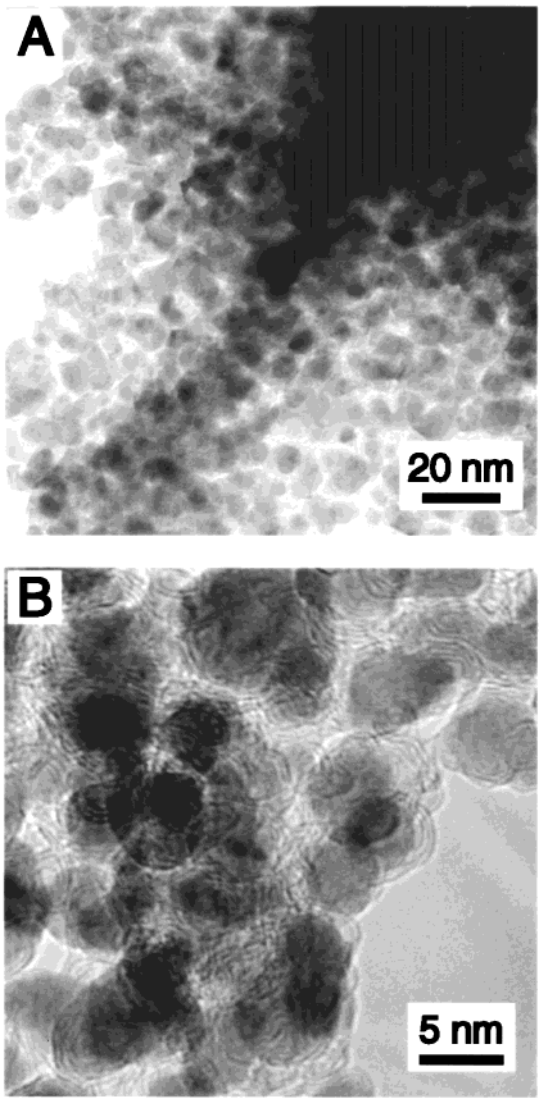

Figure 3. (A) A TEM image of the wall structure of 3DOM Co heated in nitrogen at 300 °C for 3 h and then at 400 °C for 3 h. (B) Graphitic carbon layers are visible around the Co grains (dark areas) in this TEM of the same sample taken at higher magnification.

sphere. The oxalates of these metals decompose thermally according to the reaction:

$$MC_2O_4 \rightarrow M + 2CO_2$$

Figure 2 shows SEM images of 3DOM Ni and Co metal calcined in N_2 at 450 °C for 1 h. In both samples, it can be seen that periodic air spheres are surrounded by smooth spherical walls, which are interconnected through windows and form 3D macroporous structures. Average pore diameters of 320 ± 6 nm (Ni) or 330 ± 8 nm (Co) were obtained with 410 ± 10 nm PMMA spheres. Typically, the wall thickness is less than 40 ± 5 nm. TEM images of the wall structure of 3DOM Co (Figure 3) show that the walls are composed of grains with sizes of 5−10 nm. The texture of the wall structure was studied by nitrogen adsorption measurements. Both 3DOM Ni and 3DOM Co samples exhibited a type II nitrogen adsorption isotherm with BET surface area of about 160−175 m^2/g. The high surface area is mostly due to the smaller grain size (with some contributions from residual carbon, see below) and comparable to the surface area of microporous metals, such as Raney nickel. Because of the large surface area, the 3DOM metals are highly reactive. A fresh sample may combust upon rapid exposure to air at room temperature. By controlled oxidation in a mixture of air (0.2 L/min) and nitrogen (1.0 L/min) for 30 min to passivate the sample surface, air-stable products were obtained.

By powder XRD characterization, the phases of the crystalline components in both samples could be identified as pure metals (PDF no. 04-0850 for Ni and PDF no. 15-0806 for Co). Figure 4a shows the XRD pattern of 3DOM Ni as an example. Because of the small grain size, the peaks are broadened. On the basis of the full width at half-maximum (fwhm) of diagnostic XRD peaks, the average grain size is 4.6 ± 0.3 nm, consistent with TEM observations. Although an X-ray energy dispersive spectrum (XEDS) of this sample shows the presence of some oxygen, no reflections due to oxide were observed in the XRD pattern, indicating that the amount of oxide was small and probably in amorphous

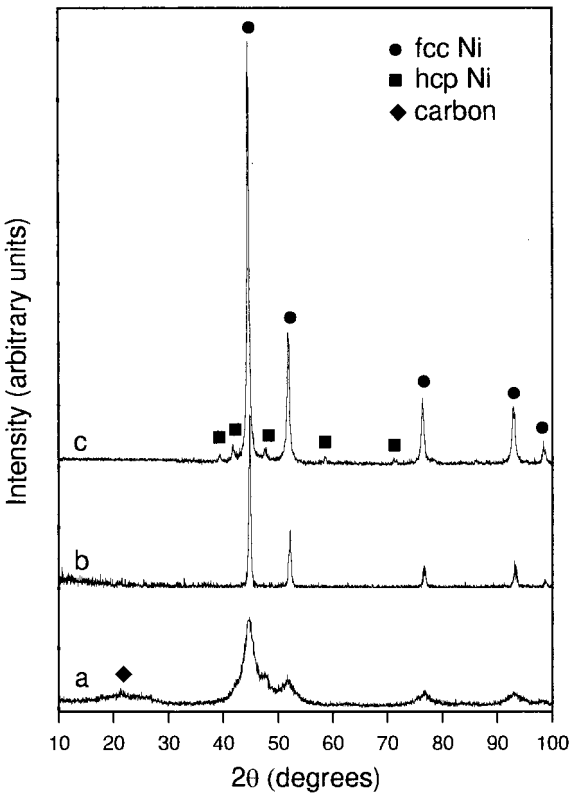

Figure 4. Powder XRD patterns of 3DOM Ni (a) prepared by calcination in N_2 at 450 °C for 1 h, (b) prepared by reduction of 3DOM NiO in H_2 at 300 °C for 2 h, and (c) prepared by direct calcination in H_2 at 400 °C for 1 h. A weak, broad diffraction peak attributed to residual carbon is marked with (◆) in curve (a). In curve (c), diffraction lines corresponding to fcc Ni are marked with (●), lines corresponding to hcp Ni with (■).

form. A broad, weak reflection in the 2θ region between 20° and 30° is attributed to amorphous carbon due to the incomplete decomposition of PMMA spheres. Carbon analysis shows that the products contain about 10−15 wt % carbon, a much lower amount than in similar materials prepared with a PS template. For example, in a macroporous Ni/PS sample, 39 wt % carbon remained after heating in nitrogen at 450 °C for 10 h. A high-resolution TEM image of a 3DOM Co sample obtained with a PMMA template (Figure 3B) indicated that the carbon existed as a coating on the metal surface. In the image, the dark circular shapes are grains of cobalt metal. Each grain is surrounded by several layers spaced a little more than 0.3 nm apart, consistent with pyrolitic graphite, which may keep the metal grains separate and prevent them from growing larger during calcination.[22]

2. Reduction of 3DOM Metal Oxides. An alternate method of synthesizing 3DOM metals involves the reduction of preformed 3DOM metal oxides.[4] This approach has also been applied to the synthesis of a 3DOM semiconductor from its oxide.[8] Figure 5 shows the SEM and TEM images of 3DOM Fe metal prepared by heating 3DOM Fe_2O_3[17] in H_2 at 300 °C for 2 h. The porous nature and periodicity of the structure were largely maintained after reduction. The rodlike morphology of the wall skeleton is due to enhanced sintering of the grains compared to samples prepared in nitrogen (compare, for example, the insets in Figures 5A and 2A). A close-up look at the walls of 3DOM Fe using TEM shows the core and shell appearance of the grains. Analysis of selected area electron diffraction (SAD) patterns indicates the presence of an iron oxide shell around an α-iron core, resulting from oxidation of the iron metal upon exposure to air after calcination.[22]

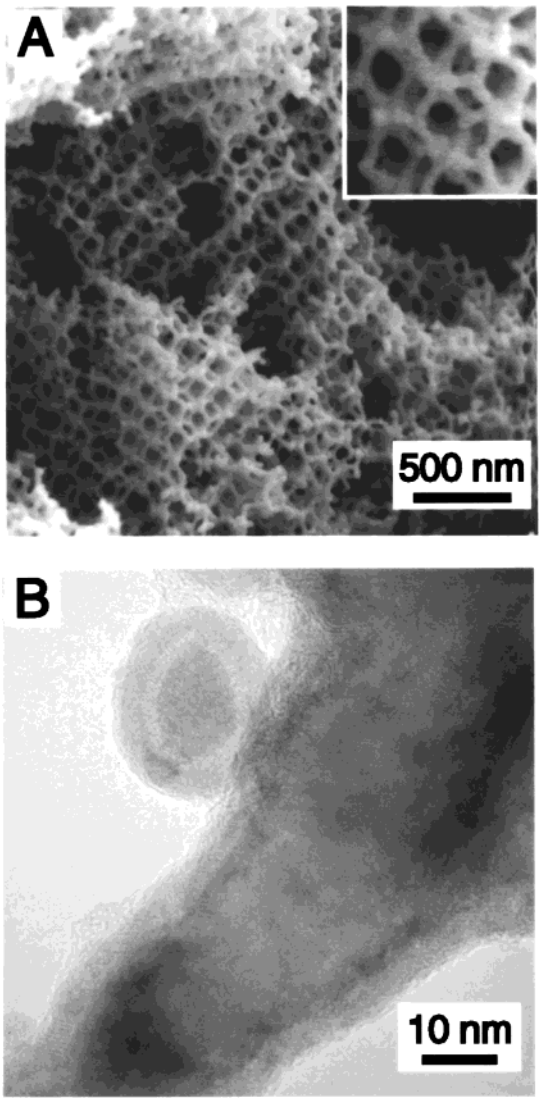

Figure 5. (A) SEM image of 3DOM Fe prepared by reduction of the 3DOM oxide in H_2 at 300 °C for 2 h. The inset shows an enlarged area to illustrate the rodlike skeleton that forms the pore structure in this sample. (B) TEM image of the same sample showing the core−shell structure of the grains and walls (see text).

The pore diameters (based on center-to-center measurements, which coincide with distances between opposite windows in one macropore) were considerably smaller than the original diameters of 3DOM metal oxides, and the walls were thicker. For example, in one batch of 3DOM nickel, the pore diameter was only 170 ± 10 nm after reduction of 3DOM NiO with a pore size of 270 ± 10 nm, and the wall thickness increased to 60 ± 5 nm from an original thickness of 35 ± 5 nm. Most carbon from the PMMA template was removed by calcination in air during the preparation of the 3DOM metal oxide precursor, so that the carbon content in the

(22) Blanford, C. F. Ph.D. Thesis, University of Minnesota, Minneapolis, 2000.

final metallic products was low (see Table 2). XRD patterns showed only diffraction lines corresponding to the metal; no carbon or metal oxide reflections were present. For 3DOM Co, a minor component of hcp cobalt (PDF no. 05-0727) was found in the product in addition to the major fcc phase (PDF no. 15-0806), probably due to fast cooling after reduction. Moreover, the diffraction lines corresponding to the metal are sharper and more intense (Figure 4b) compared to the samples calcined in N_2, consistent with the larger size of the metal grains. On the basis of the fwhm of diagnostic diffraction peaks, the average grain sizes of the 3DOM metals ranged from ca. 20 to 40 nm. Larger grains were also observed in the TEM. Because of the grain growth, the BET surface areas of the 3DOM metals were reduced accordingly, ranging from 5 to 17.9 m^2/g.

It should be noted that the reduction conditions used here were optimized conditions. A lower reducing temperature (250 °C, 2 h) or a shorter time (300 °C, 1 h) resulted in incomplete reduction, and hence the metal and metal oxide coexisted in the product. In addition, these reduction conditions are milder than traditional temperatures used for the reduction of bulk metal oxides, which range from 360 to 700 °C for Ni, Co, and Fe.[23] For comparison, in this study, when a commercial Fe_2O_3 powder (Aldrich, nonmacroporous, grain size <5 μm) was exposed to H_2 at 300 °C for 2 h, only a mixture of Fe_3O_4 (main phase) and Fe metal (secondary phase) was obtained. It is postulated that the different behavior is related to the highly accessible framework, thin walls, and small grain size of the 3DOM structure. Free transport of H_2 and short ion diffusion lengths in 3DOM structures greatly facilitate the H_2 reduction process and other interfacial reactions.

3. Template Removal in H_2. To develop a more convenient route toward 3DOM metals, the combined processes of metal oxalate reduction and PMMA template removal in a hydrogen atmosphere were investigated. Figure 6 shows the SEM images of 3DOM Ni and Fe metal heated in H_2 at 400 °C for 1 h. Again, ordered macroporous structures were obtained. Compared with 3DOM metals prepared by metal oxide reduction, the products heated directly in H_2 contained larger ordered domains, indicating less structural degradation during the calcination. Using 410 nm sphere templates, average void spacings were 298 ± 10 nm for 3DOM Ni and 220 ± 8 nm for 3DOM Fe. (For comparison, 3DOM Fe prepared via the oxide from the same templates exhibited average void spacings of 185 ± 8 nm.) Many regions were visible in the wall structure where spherical grains had aggregated, forming a textured skeleton (see inset in Figure 6A). The diffraction peaks in the XRD patterns of the 3DOM Fe and Ni samples corresponded to the cubic metal phases (bcc for Fe, fcc for Ni), although a small amount of an additional hcp phase was found for the Ni sample (Figure 4c). The BET surface areas were larger than those of metal samples prepared by the reduction method, ranging from 10 to 33 m^2/g.

Elemental analyses indicated that the carbon content in all these samples was less than 2 wt %, i.e., much lower than by calcination in a nitrogen atmosphere. The carbon elimination process is believed to benefit from the catalytic properties of the transition metals in the wall skeleton. It is well-known that many transition metals (such as Ni, Co, and Fe) can absorb hydrogen.[24] When hydrogen is adsorbed on the metal surface, some hydrogen molecules can be activated and attack a carbon−carbon bond of an adsorbed polymer chain.[25] This hydrogenolysis process leads to a chain scission reaction that enhances the degradation of PMMA. For this reason, the PMMA can decompose more quickly and completely in the presence of a transition metal in a hydrogen atmosphere.

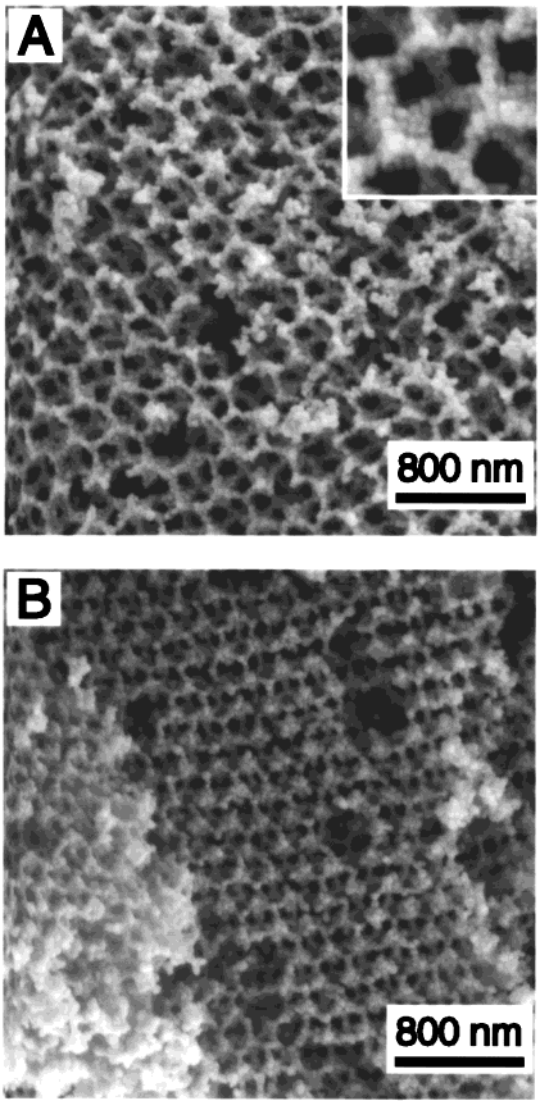

Figure 6. SEM images of (A) 3DOM Ni and (B) 3DOM Fe prepared by direct calcination in H_2 at 400 °C for 1 h. The inset in image (A) shows similar skeletal features to those seen in Figure 5A, but with a more textured appearance.

Preparation of 3DOM Alloys. The above strategy can be conveniently applied to synthesize 3DOM alloys from mixed oxalate precursors.[13] As a demonstration, $Ni_{1-x}Co_x$ alloys with ordered arrays of macropores were prepared at different Ni:Co ratios. In the compositional range examined here, $Ni_{1-x}Co_x$ systems form solid−

(23) Nicholls, D. In *Comprehensive Inorganic Chemistry;* Bailar, J. C., Emeléus, H. J., Sir Nyholm, R., Trotman-Dickenson, A. F., Eds.; Pergamon Press: Oxford, 1973; Vol. 3, pp 982, 1054, 1110.

(24) Bhatia, S. *Zeolite Catalysis: Principles and Applications*; CRC Press: Boca Raton, FL, 1989.

(25) Gates, B. C.; Katzer, J. R.; Schuit, G. C. A. *Chemistry of Catalytic Processes*; McGraw-Hill: New York, 1979; pp 274−275.

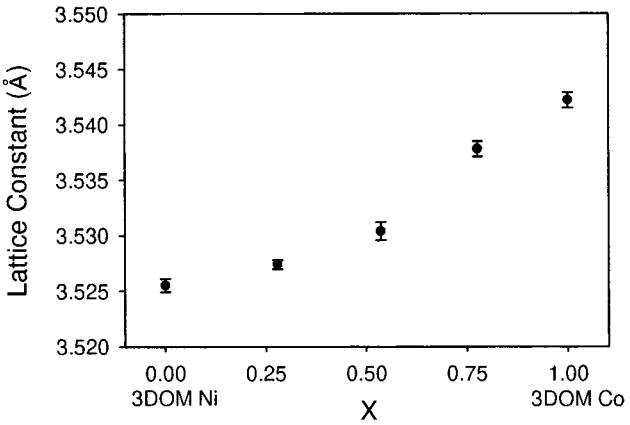

Figure 7. Variation in lattice constant for the wall grains of 3DOM $Ni_{1-x}Co_x$ with mole fraction of Co (x).

solution alloys, and XRD patterns of the 3DOM alloys were consistent with the fcc structure ($Fm3m$) observed for the bulk alloy.[26] Figure 7 shows the variation in lattice constant vs X for 3DOM $Ni_{1-x}Co_x$ samples that were synthesized under identical conditions. The relatively smooth increase in lattice constant at increasing Co content confirms substitution of Co for Ni in the solid solution. Other structural and compositional features, such as grain size, BET surface area, and carbon content, are similar to those of metals synthesized by calcined in H_2 (see Table 2).

Conclusions

Colloidal crystal-templated precipitation and subsequent chemical conversion is a general method for the fabrication of 3DOM metal oxides and carbonates,[17] metals, and alloys. This study showed that in the preparation of 3DOM metals or alloys, the choice of template, reduction procedure, temperature, and atmosphere play significant roles in determining the size of macropores, structural order, wall thickness, grain size, phase purity, and surface area of the products. PMMA colloidal crystal templates permit lower temperature processing than PS templates. 3DOM metals prepared in N_2 have highly ordered macroporous structures, high surface areas (>160 m^2/g), and small grain sizes (<10 nm); however, more than 10 wt % carbon typically remains in the product. By reducing 3DOM metal oxides in H_2, carbon can be completey eliminated, but the order of the structure diminishes due to large volume shrinkage. In addition, the surface area of the products is significantly lower (5−18 m^2/g). Direct calcination in H_2 may be a compromising strategy. Relatively little carbon (<2 wt %) remains in the products; on the other hand, the 3DOM products have greater structural order and higher surface areas (10−30 m^2/g). The versatility of this synthetic procedure combined with various posttreatments can greatly expand the varieties of accessible 3DOM compositions, which include Fe, Ni, Co, and other metals whose salt precursors are easily reducible and whose melting points exceed that of the template. By controlling synthesis conditions, it is possible to tailor compositions, macrostructures, and microstructures according to specific requirements. As a result, the class of metals and alloys presented here may find applications as high-performance catalysts, electrodes, supports, and magnetic materials. Further research on the physical, chemical, and electrochemical properties of these porous metals is underway.

Acknowledgment. We thank 3M, Dupont, the David and Lucile Packard Foundation, the McKnight Foundation, the University of Minnesota Center of Interfacial Engineering, the National Science Foundation (DMR-9701507 and the MRSEC program of the NSF under Award DMR-9809364), and the Department of Energy (DOE/DE-FG02-93-ER14384) for support of this research. J.C.L. acknowledges the NSR-REU program for summer support. The IT Characterization Facility is gratefully acknowledged for use of the SEM, TEM, and XRD facilities.

CM0105716

(26) Nishizawa, T.; Ishida, K. In *Binary Alloy Phase Diagrams*, 2nd ed.; Massalksi, T. B., Ed.; ASM International: Materials Park, OH, 1990; Vol. 2, pp 1214−1215.